Fragmentation of molecules by fast ion impact

C Dimopoulou[1,2], N Haag[1], R Moshammer[1], P D Fainstein[3],

A Dorn[1], M Dürr[1], D Fischer[1] and J Ullrich[1]

[1]Max-Planck-Institut für Kernphysik, Saupfercheckweg 1, 69117 Heidelberg, Germany

[2]Gesellschaft für Schwerionenforschung, Planckstr. 1, 64291 Darmstadt, Germany

[3]Centro Atómico Bariloche, Comisión Nacional de Energía Atómica, 8400 Bariloche, Argentina

c.dimopoulou@gsi.de

Abstract. Single ionization of simple molecules, e.g. H_2, CO_2, by fast charged particle impact has been studied using a reaction microscope. By measuring the momenta of the emitted electron and the recoil ionic fragment in coincidence, channel-selective low-energy electron spectra have been recorded. The experimental cross sections will be presented, compared with the predictions of state-of-the-art CDW-EIS calculations and discussed in terms of molecular effects such as (i) autoionization and predissociation channels, (ii) interference patterns resulting from the two-center geometry of the diatomic molecule, in analogy to Young's double-slit experiment and (iii) dependence of the electron emission on the orientation of the molecular axis.

1. Introduction

Systematic highly differential studies of fragmentation of simple molecules by fast ion impact have been performed. Molecular hydrogen and carbon dioxide have been chosen as benchmarking systems for fundamental studies as well as for medical applications. Particular attention is given to the emission characteristics of the low-energy electrons, which are very reactive in biological tissue [1].

Two possible pathways can be distinguished in single ionization of H_2. First, a stable, possibly vibrationally excited H_2^+ ion remains after the removal of the electron (non-dissociative ionization: (1) in figure 1). Second, in a few percent of all ionization events [2], the molecule dissociates into a H^+ ion and a H atom (dissociative ionization). The latter happens either by the creation of an excited molecular ion which dissociates since all $(H_2^+)^*$ states are repulsive in the Franck-Condon region or by populating the vibrational continuum of the ground state of H_2^+, resulting into dissociation into a H^+ and a H(1s) (ground state dissociation: (2) in figure 1). The kinetic energy of the H^+ from ionization plus excitation is typically of the order of a few eV, whereas from ground state dissociation it is in the sub-eV range [3]. In addition, double excitation of H_2 into autoionizing states contributes within a few percent to the dissociative ionization [2, 4]. Here, we are concerned with ground state dissociation (GSD) since in our experiment we have detected very low-energy (< 40 meV) H^+ ions.

Similarly, in single ionization of CO_2, either a stable, possibly electronically and/or rovibronically excited $CO_2{}^+$ ion remains (non-dissociative ionization): (a) $CO_2 \rightarrow CO_2^+$ [or $(CO_2^+)^*$] $+ e^-$ or the molecule dissociates into a charged and a neutral fragment (dissociative ionization): (b) $CO_2 \rightarrow CO^+ + O + e^-$ or (c) $CO_2 \rightarrow O^+ + CO + e^-$.
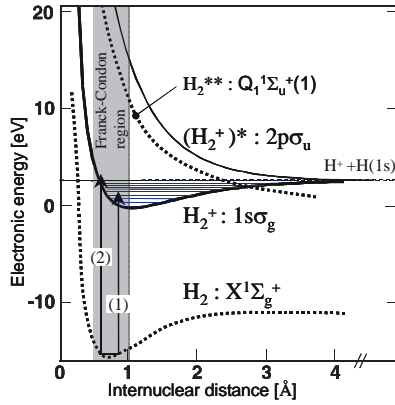

Figure 1. Schematic potential curves for H_2 and $H_2{}^+$ illustrating the single ionization pathways.
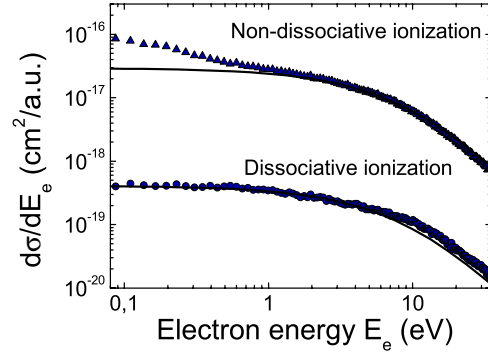

Figure 2. Electron energy distributions for single ionization of H_2 by 6 MeV proton impact. Triangles: non-dissociative ionization. Circles: dissociative ionization. Solid lines: CDW-EIS results.

Single ionization of H_2, CO_2 by fast proton impact has been studied by measuring in coincidence the momentum vectors of the emitted electron and the charged nuclear fragment. For non-dissociative ionization the measurement represents a kinematically complete experiment, since the momentum transferred by the projectile can be reconstructed event by event by the measured momenta of the electron and the recoil ion, whereas this is not the case for dissociative ionization because the neutral atomic fragment is not detected. Thus, we have recorded electron energy spectra resolved down to 0.1 eV for all reaction pathways. In addition, fully differential cross sections (FDCS) have been obtained for non-dissociative ionization.

The experiment was performed at the Tandem accelerator of the Max-Planck-Institute for Nuclear Physics in Heidelberg using a "Reaction Microscope" [5]. A well-collimated, pulsed, 6 MeV proton beam crosses a molecular gas jet. The target molecules (H_2, CO_2) are in the vibrational ground state, since they reach a temperature of less than 10 K after the supersonic expansion. The emitted electrons and the recoil ions are extracted into opposite directions along the projectile beam axis (longitudinal direction) by a weak (4.5 V/cm) electric field over 11 cm and detected by two-dimensional position sensitive detectors. A uniform longitudinal magnetic field of 14 G confines the transverse motion of the electrons, such that all electrons with energy $E_e < 35$ eV are detected with the full solid angle. The momentum vectors of both, recoil ion ($H_2{}^+$ or H^+; $CO_2{}^+$ or CO^+ or O^+) and electron, are determined from their measured absolute times-of-flight and positions on the detectors (details in [6-8]).

A continuum-distorted-wave eikonal-initial-state (CDW-EIS) model [9, 10] has been developed in order to describe electron emission in non-dissociative ionization of H_2. Briefly, the initial state of H_2 is approximated by a superposition of two hydrogenic orbitals centered at each nucleus with a separation given by the equilibrium internuclear distance (R = 1.4 a.u.) and an effective charge of Z_{eff} = 1.19 to correctly reproduce the electronic binding energy. The resulting FDCS for emission of an electron with momentum vector $\mathbf{p_e}$ in a collision where the momentum transfer is $\mathbf{q}$, is equal to the one for ionization of two "effective" H atoms multiplied by the oscillatory term $1 + \cos\left[(\mathbf{p_e} - \mathbf{q}) \cdot \mathbf{R}\right]$. The

latter represents the interference caused by the coherent electron emission from the two H centres for a fixed orientation of the molecular axis $\mathbf{R}$. Averaging over all molecular orientations, the corresponding interference term is $(1+\sin\chi/\chi)$, $\chi \equiv |\mathbf{p_e} - \mathbf{q}|R$. The motion of the nuclei in H_2 is not taken into account in this model.

2. Channel-selective low-energy electron spectra

2.1. Vibrational autoionization in H_2

In figure 2 the electron energy distributions for both fragmentation pathways are compared with the CDW-EIS results. First, the data from pure ionization are in reasonable agreement with the CDW-EIS calculation except for $E_e < 1$ eV where a significant enhancement of the cross section is observed (feature I). Second, at E_e around 12 eV a distinct difference appears in the shape of the cross sections between the CDW-EIS and the dissociative ionization (feature II).
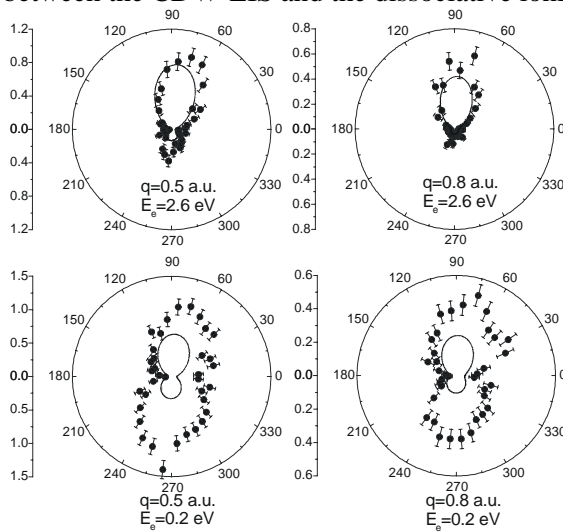
Figure 3. FDCS for electrons emitted into the scattering plane for non-dissociative ionization of H_2 by 6 MeV proton impact. Upper row: The electron energy $E_e = 2.6$ eV is fixed and the values of the momentum transfer are q = 0.5, 0.8 a.u.. Lower row: $E_e = 0.2$ eV, same values of q. Solid lines: CDW-EIS results. The cross sections are given in 10^{-18} cm^2/au^2.

The feature I is due to the autoionization of rovibrational levels of singly excited bound Rydberg states of H_2 [6]. The electronic curves of these states lie within a few eV below the ground state of H_2^+ ($1s\sigma_g$ in figure 1) and are essentially parallel to it, whereas their higher vibrational levels have energies above the ionization potential of H_2 and therefore autoionize by converting energy from the vibrational motion into kinetic energy of the outgoing electron. The electron can be viewed to autoionize by scattering on the ion core. The differences between this vibrational autoionization and the direct ionization to the continuum become evident in the FDCS at E_e above and below about 2 eV. As expected for the directly ionized electrons ($E_e = 2.6$ eV, upper row in figure 3) the data agree well with the CDW-EIS on an absolute scale. The large peak (binary peak) in the direction of the momentum transfer $\mathbf{q}$ (practically at 90°) corresponds to electrons ejected by a binary interaction with the projectile, whereas the smaller peak in the direction of $-\mathbf{q}$ (recoil peak) corresponds to the case when most of the momentum transfer is taken by the recoil ion. As q increases the recoil peak systematically decreases in magnitude relative to the binary peak. However, for the very low-energy electrons ($E_e = 0.2$ eV, lower row in figure 3), the ratio between the recoil and the binary peak is close to one and does not change with increasing q, a feature that can be understood for vibrational autoionization: Making use of the analogy between charged particle impact excitation (ionization) and photoionization for small q and E_e [11], we expect that the angular distribution of the autoionized electrons is essentially a dipolar one with respect to the momentum transfer axis. In fact, the autoionization can be described as a dipole-like photoexcitation of the molecule to a bound intermediate electronic state, followed by a transition of the electron into a continuum p-state after transfer of energy from the vibrating nuclei to the electron, leaving the H_2^+ ion in its $1s\sigma_g$ ground state.

The feature II that appears in the dissociative ionization can be explained by the contribution of an additional channel, namely the excitation of a doubly excited Rydberg state of H_2 autoionizing into the vibrational continuum of the ground state of H_2^+ (figure 1):

$$H_2\left(X\,^1\Sigma_g^+\right) \to H_2^{**}\left(Q_1\,^1\Sigma_u^+(1)\right) \to H^+ + H(1s) + e^- \text{ [4, 6]}.$$

2.2. Predissociation in CO_2

What is the mechanism leading to the dissociative ionization of CO_2? From figure 4 and the known Franck-Condon factors [12] it is evident that the dissociation limits of the CO_2^+ states X, A, B, C are not directly accessible by vertical transitions from the ground state of the molecule. However, we have measured a significant contribution of the dissociative ionization channels (b) and (c) (see section 1) [8]. Indeed, the dissociation takes place indirectly, by the predissociation mechanism, which is schematically shown as transition (1) in figure 4. With a certain probability, during the collision the CO_2 molecule is ionized and simultaneously excited to the state C $^2\Sigma_g^+$. This state lies above the dissociation limit of CO_2^+ and, within a very short time in comparison to the lifetime of radiative decay, undergoes a curve crossing (via coupling to another molecular state) into the dissociation continuum at 19.1 eV, leading to the fragments $O^+ + CO$. Similarly, fragmentation into $CO^+ + O$ takes place by predissociation of vibrationally excited levels of C $^2\Sigma_g^+$ which lie above the $CO^+ + O$ dissociation limit, as depicted by transition (2) in figure 4. This interpretation is supported by photoionization studies of CO_2 [8, 13].
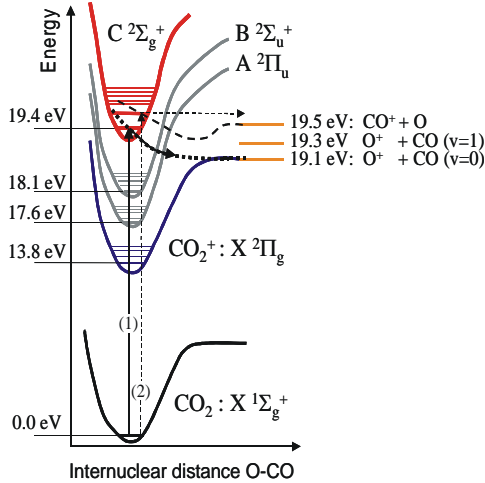

Figure 4. Schematic potential curves for CO_2 and CO_2^+ with the lowest dissociation limits of CO_2^+. The suggested mechanism for $CO_2 \to O^+ + CO + e^-$ by predissociation (curve crossing) of the C $^2\Sigma_g^+$ state of CO_2^+ is illustrated by (1). For $CO_2 \to CO^+ + O + e^-$ the analogous mechanism is shown by (2).
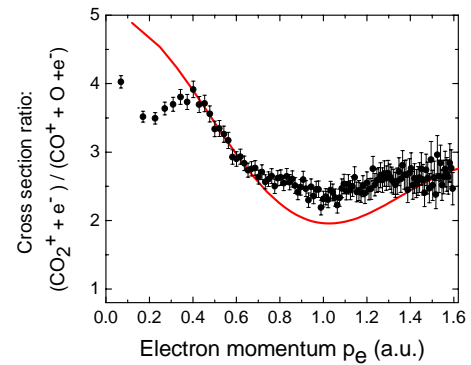
Figure 5. Ratio of the electron momentum distribution for non-dissociative single ionization of CO_2 to the one for fragmentation into $CO^+ + O$. Solid line: calculation of the simple interference term $\left[1 + \sin(p_e\,R)/(p_e\,R)\right]$ with R= 4.38 Å, scaled on the data at p_e=0.4 a.u.

3. Interference effects in fragmentation of CO_2 ?

In a simplified geometrical "two-slit" picture, we can in principle expect interference effects because the detected electron was emitted from one or the other O atom of CO_2. Since CO_2 is a linear molecule, the relevant "two-slit" separation is equal to twice the C-O bond length i.e. R= 4.38 Å, which is larger than the de Broglie wavelength of the emitted low-energy electron. Such interference effects can be probed by comparing directly the measured spectra for electrons coincident with CO_2^+ ions i.e. emitted coherently from the two O atoms, to those for electrons emitted in the $CO^+ + O$

fragmentation channel where the two O atoms are distinguishable. In figure 5 we have plotted the ratio of the electron momentum distribution from channel (a) to the one from channel (b), in comparison with the simple oscillatory function $[1 + \sin(p_e\,R)/(p_e\,R)]$, which represents the interference caused by the two O centers for random orientation of the O-C-O axis [14]. A good qualitative agreement in the period of the oscillation in the cross section ratio is observed. However, quantitative conclusions cannot be drawn since additional molecular channels are superimposed on the electron spectra.

4. Electron emission in the frame of the H_2 molecule

If the dissociation of the molecule is fast compared with its rotation, then the direction of the emitted nuclear fragments corresponds to the initial orientation of the molecular axis during the collision (axial recoil approximation [15]). Within this approximation and taking into account the complications resulting from the collision kinematics in our kinematically non-complete experiment [7], we have obtained, in the case of GSD of H_2, molecular-frame electron angular distributions for molecules oriented perpendicular to the projectile beam. They are plotted in figure 6 in the plane defined by the incoming projectile and the detected H^+ fragment, as a function of the polar electron emission angle relative to the initial projectile direction, for E_e= 2.5 eV, 10 eV and 20 eV. They are compared in shape to the predictions of the CDW-EIS model for a fixed orientation of the molecular axis as described above ("molecular" calculation: solid lines) as well as for two "effective" H atoms, i.e. without the interference term ("effective" atomic calculation: dashed lines). The small structures appearing in the "molecular" calculation mainly in the forward and backward directions essentially result from the interference term and are important as the de Broglie wavelength of the emitted electron becomes comparable to the internuclear distance [10]. For the low E_e considered here, they are very small. Within statistical errors the data agree well with both, "effective" atomic and "molecular", calculations, so that our experiment cannot provide evidence for interference patterns. Another question is whether they exist at all for dissociative ionization where we actually distinguish the two nuclear centres by knowing the emission direction of the H^+ ion.
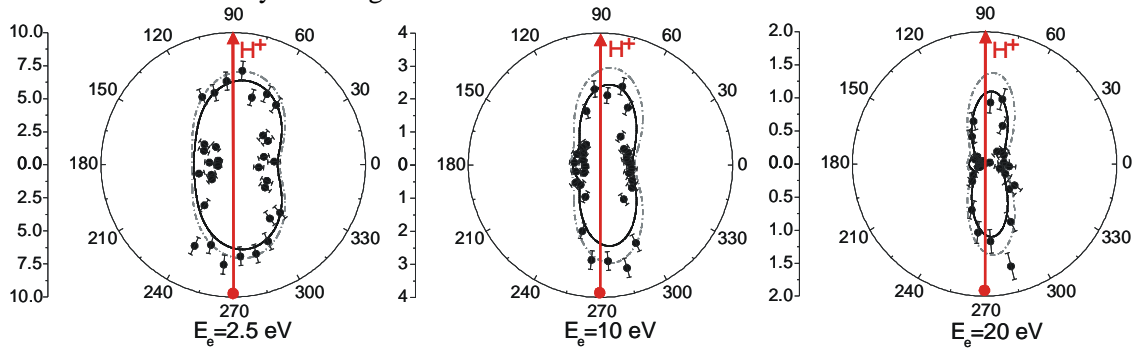
Figure 6. Electron angular distributions for H_2 molecules oriented perpendicular to the incoming projectile beam and for E_e= 2.5 eV, 10 eV and 20 eV. The arrows indicate the emission direction of the detected H^+ fragment. CDW-EIS calculation: "molecular" (solid lines), "effective" atomic (dashed lines). The theoretical FDCS have been integrated over $\mathbf{q_\perp}$. The cross sections are given in 10^{-20} cm^2/eV. The data have been normalised to the "molecular" CDW-EIS cross section around 90°.

5. Kinematically complete dissociative ionization of H_2 by electron impact

In fast ion collisions the deflection angle of the projectile is undetectably small (nrad-µrad). However, for electron impact it is measurable due to the lower electron mass. Very recently, it was possible to perform a first kinematically complete experiment on ground state dissociation of H_2 by 210 eV electron impact, using an advanced reaction microscope (details in [16]), where the scattered projectile electron is detected in coincidence with the emitted electron and the H^+ fragment [17]. Thus, the momentum transfer $\mathbf{q}$ is determined and the dependence of the cross section on the molecular orientation can be studied in the scattering plane, as shown in figure 7. The cross section is anisotropic

and shows a maximum for molecules oriented along the axis of the momentum transfer and a minimum perpendicular to it. Detailed studies are underway in order to interpret this effect.
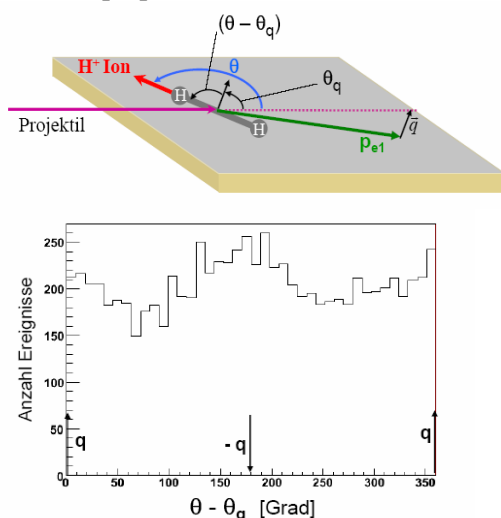

Figure 7. Kinematically complete ground state dissociation of H_2 by 210 eV electron impact. Illustration of the scattering plane i.e. defined by the momentum vectors of the incoming and scattered projectile. The emission direction of the H^+ ion lies in the scattering plane and corresponds to the orientation of the molecular axis during the collision. Dependence of the cross section on the relative angle between momentum transfer and H^+ fragment (molecular axis) in the scattering plane.

6. Conclusions

In summary, the channel-selective electron spectra from single ionization of H_2 and CO_2 by 6 MeV proton impact provide evidence that purely molecular channels affect significantly the emission of low-energy electrons. In particular, the vibrational autoionization, which is an explicit example of the break-down of the Born-Oppenheimer approximation, gives a sizeable (more than 10%) contribution to the total single ionization cross section of H_2. Our data reveal the importance of the collision-induced excitation of the molecule into channels which undergo radiationless decay, via autoionization and also via predissociation. Within the axial recoil approximation, we obtained, molecular-frame electron angular distributions in a kinematically non-complete experiment on fast ion-impact dissociative ionization of H_2. In recent kinematically complete electron-impact studies an anisotropy in the molecular-orientation dependence of the dissociative ionization cross section has been observed.

References
[1]   Boudaiffa B et al 2000 Science **287** 1658
[2]   Ben-Izthak I *et al* 1996 *J. Phys. B: At. Mol. Opt. Phys.* **29** L21-L28
[3]   Edwards A K, Wood R M, Beard A S and Ezell R L 1990 *Phys. Rev.* A **42** 1367
[4]   Wood R M, Edwards A K and Steuer M F 1977 *Phys. Rev.* A **15** 1433
[5]   Ullrich J *et al* 2003 *Rep. Prog. Phys.* **66** 1463
[6]   Dimopoulou C *et al* 2004 *Phys. Rev. Lett.* **93** 123203
[7]   Dimopoulou C *et al* 2005 *J. Phys. B: At. Mol. Opt. Phys.* **38** 593
[8]   Dimopoulou C *et al* 2005 *J. Phys. B: At. Mol. Opt. Phys.* **38** 3173
[9]   Galassi M E, Rivarola R D, Fainstein P D and Stolterfoht N 2002 *Phys. Rev.* A **66** 052705
[10]   Laurent G et al 2002 *J. Phys. B: At. Mol. Opt. Phys.* **35** L495
[11]   Inokuti M 1971 Rev. Mod. Phys. **43** 297
[12]   Sharp T E and Rosenstock H M 1964 J. Chem. Phys. **41** 3453
[13]   McCulloh K E 1973 J. Chem. Phys. **59** 4250
[14]   Cohen H D and Fano U 1966 Phys. Rev. **150** 30
[15]   Zare R N 1967 J. Chem. Phys. **47** 204
[16]   Dürr M, Dimopoulou C, Najjari B, Dorn A and Ullrich J 2006 Phys. Rev. Lett. **96** 243202
[17]   Haag N 2006 Diploma Thesis University of Heidelberg (in german)